International Journal of Civil and Structural Engineering – IJCSE
Copyright © Institute of Research Engineers and Doctors
Volume 6 : Issue 2 - [ISSN : 2372-3971] - Publication Date: 27 Dec, 2019

Seismic Behavior of Vestas Wind Turbine Tower Including Dynamic Soil Structure Interaction

at *Zafarana Wind Turbine Farm, Egypt*

Abdelrahman, G. E[1], Youssef, Y. G[1], Abdelaziz, M.H[1], Mohamed, K. I[1*]

***Abstract*—** Due to the rapid expansion of wind energy and the growing numbers of wind turbines constructed in earthquake areas. It is required to perform more research works for a better understanding of this issue. Accordingly, this humble study is needed. This study considered the onshore Vestas (V47/660) wind turbine tower which is located at Zafarana Wind Turbine Farm in Egypt. The foundation of this tower is designed as a large rigid reinforced concrete type and constructed in an active seismic region. The main research question is; what is the effect of the soil type, seismic frequency and amplitudes on the foundation and the tower translation movement? Also, the research hypothesis believes that the softer the soil is the greater its effect on tower and foundation deformations. Accordingly, this study has been planned. The aerodynamic effect induced due to the turbine blades has been excluded, while the static loads of the turbines as well as the seismic effect of the regions have been considered. That is to say, the study considered the at rest cases of loading. However, two-time history moods of different earthquakes have been investigated. The foundation soil has been changed two times to investigate its effect. This research could be classified as a numerical study based on finite element analysis in the three dimensions, i.e. 3D. Then, Plaxis 3D-2017, license dynamic VIP version has been used to accomplish the main part of this study. It has been concluded that as the fundamental frequency of the earthquake gets closer to the natural frequency of the soil or the tower, the deformations within soil, footing and tower body will dramatically increase. Moreover, the hypothesis believes previously assumed are found to be true.

***Keywords*—**wind turbines, earthquake, dynamic soil structure interaction, plaxis 3d.

I. Introduction

Wind turbine structures have the most common tall and slender geometric forms and have a heavy turbine on the top of tower The structural characteristics determined their seismic response should be influenced by wind turbine operational state soil structure interaction There are several current important standards have simple actions for assessing earthquake loading based on one degree of freedom and site design acceleration response spectra Because ignoring high models the soil structure interaction is not included in these simple procedures which may lead the seismic load calculated following the current standards is not accurate The purpose of this study is to examine the structural dynamic response of different types of wind turbine towers foundation at Zafarana Wind Farm to consider the Soil Structure Interaction (SSI).

Electricity from wind power becomes one of the most effective solutions to overcome the increasing demand of electricity and shortage the sources. The electricity power from wind energy becomes more than 539 GW in 2017 according to [1]. The Egyptian government seeks to improve its electricity capacity from renewable energy such as solar, wind and hydro energy to reach 20% of the total electrical power by 2022. The 20 percent will be distributed to renewable energy sources as follows, 12% for wind power, 6% for hydro sources and 2% for solar energy. As a result, the Egyptian government pays great attention to increase its electricity production through wind energy, thus the production of wind energy will reach 7.2 GW by 2022. The wind power productivity in Egypt jumps up from 5 MW in 2001 to 810 MW in 2017. The wind speed requirement to build wind turbine farms is more than 6 m/s to allow the blades of the turbine to move and generate electricity. Therefore, the Gulf of Suez in Egypt enjoys a large wind speed with an average annual wind speed of ten and a half meters per second. The budget that was invested in renewable power in Egypt reach 2.6 billion dollars by the end of 2017.

The research on Earthquake act of wind turbines, that it's foundation is shallow, is relatively new. The mechanical parts in wind turbine towers are shafts, bearings, gears and links. All of these parts should be work well and normally after the seismic excitation. For the normal operation continuity, the deformations and/or tilting at the top of towers should not exceed the serviceability limit state. Generally, the natural frequency of wind turbine towers is less than any structure that has the same height. The mass of blades, hub, rotor and nacelle at the top of turbine tower could be the same as the mass of the tower itself that leads to short in the natural frequency. As the properties of the wind turbine towers structure are different from the conventional structures, it is very important to assess the dynamic response of the wind turbine towers due to seismic action. In spite of wind turbine towers rarely collapsed due to earthquake actions [2], the normal operation of wind turbine could be affected by the seismic excitation for a significant time. So, the developers of wind power and insurance firms should take in your consideration the seismic response of wind turbines located in highly seismic zones. The main aim of this manuscript is to assess the seismic behavior of a 45 m Vestas V47/660 that is one of the wind turbines found at Zafarana wind farm, which its location 120 km in the southern direction of Suez on the Red Sea.

*Abdelrahman, G.S, Youssef, Y.G, Abdelaziz, M.H, Mohamed, K.I**
Civil Engineering Department, Faculty of Engineering/ Fayoum University
Egypt

The Zafarana wind farm is considered an active seismically zone [3]. As wind turbine towers are very expensive structure, extraordinary concern should be made to the effect of soil structure interaction. The tower foundation is a shallow square footing that is founded on two classes (i.e. soil class B and soil class c).

In this paper, the tower foundation including the surrounding soil medium are modeled using three-dimensional finite elements by Plaxis 3D. Thus, the model was excited by earthquake motion at boundary of the model (bedrock) to assess the tower seismic response at center of footing and top of tower including soil structure.

II. Previous Studies

It is extensively known that the dynamic response of the structure differs from stiff soil to softer one for the same structure exposed to the same earthquake [4]. As [5] shows the main aspects that impact the interaction between soil, foundation and the structure are layering and stiffness characteristics of the soil profile, size and flexural stiffness of the foundation, depth of foundation embedment and the inertia characteristics; slenderness and first few natural periods of the structure. SSI is ignored when the response of a structure is computed assuming the ground excitation at the foundation of structure is the same as the free-field motion [6]. The definition of free-field motion is the motion on the ground surfaces where no structure existing [7]. Such an idealization works only if the supporting medium is rigid (inflexible ground). The structures founded on weak soil, the foundation response to excitation differs from the free-field motion [8]. For flexibly supported structures significant amount of vibrational energy is dissipated into supporting medium by Radiation of elastic stress waves as they travel away from the foundation. These waves are formed by the deformation of soil due to dynamic structural forces acting on the foundation. This effect is termed as radiation damping and is 5 purely a geometric phenomenon and Inelastic behavior of the supporting soils [9]. This dissipation of energy due to hysteretic action of soils (termed as material or internal damping) depends on the level of strain induced in the soil during vibration. It is usually much smaller than radiation damping. It is analogous to structural damping and can be treated as viscous damping. It 6 is usually assumed to be 5% of critical.

There are two main approaches to solving SSI problems, the direct method and substructure approach. In the direct method, the idealized soil and structure together is studied in one step. The direct approach incomes by affecting a steady free-field ground excitation to the boundaries of a distinct model and assessing the reaction of the joined soil-structure system. Hence, a direct method determines the response of the soil and structure simultaneously [10]. Non-linear analyses are possible using the direct approach because the assumptions of superposition are not required. However, non-linear analyses can be sensitive to poorly defined soil parameters and can be computationally intensive [11]. Many studies follow the same trend that stated before for the importance of soil structure interaction especially in soft soils [12-15]. A detailed investigation of the expansion of SSI was done by [16]. There are some researches who neglected the effect of SSI during assessment the seismic response of wind turbines. [17] supposed that the wind turbine tower is founded on firm soil that has a high shearing resistance, so the soil structure interaction could be neglected. In the same way, the rigid simulation of the rigid foundation at the foundation of the tower performed by [18].

A shake table test with a full scale of a wind turbine tower 23m tested by [19] to assess the seismic response at different heights on the tower. [20] In his research on the response due to seismic excitation of tall chimneys, stated that for only the weak soil that shear wave velocity less than 750 m/s, the SSI had an effect, so this may lead to reduce or amplify in the response depending on the structure property, soil behavior and the characteristics of the earthquake. [21] noticed that ordinary soil-foundation-structure interaction (SFSI) buildups the total lateral displacement of the structure by ten to thirty percentage possibility of increasing in the structural alteration in case of considering SFSI for single degree of freedom (SDOF) structure using Monte Carlo simulations. A 5MW wind turbine tower was analyzed due to seismic loading including soil structure interaction by [22]. Previous researches [23-25] simulated the wind turbine tower with a lump mass at the top point of the tower to simulate the mass of nacelle, hub, rotor and blades. [26] showed that the difference between frequency dependent and frequency independent models is small for a specific case of a gravity base foundation for a 3 MW turbine. A comparison between flexible and fixed based foundation made by [27] and concluded that SSI has an effect on the reaction of the turbine tower due to dynamic action.

Modern wind turbines are typically installed with variable speed systems, so the rotating speed of the rotor varies from around 5-15 rpm. Therefore, the first excitation frequency range is about 0.08-0.25 Hz and is mentioned to as the 1P frequency interval. Meanwhile the first resonance frequency of a new generation of wind turbine towers, which have three blades, is always to be found between of below 1P and 3P, it is necessary to be able to determine the fundamental frequencies of the turbine towers to avoid resonance phenomena occurrence [28]. Usually foundations of wind turbine tower are simulated with fully rigid support (soil support is not taken into consideration) or let the foundation of the tower down to an equivalent fixed point (apparent fixity) or by static uncoupled springs (resulting in the foundation stiffness being frequency independent). These ideal hypotheses of the boundary conditions can underestimate the damping of the system and cause to overestimate the stiffness and so the system's natural frequency [29]. Consequently, if separation between the operational and natural frequencies is big, The fixation of the foundation should not be applied and SSI should to be considered in design [30]. It is necessary to know the structure's total natural frequency to separate its natural frequency from the rotor frequency in order to prevent resonance phenomena [31]. Along these lines, the compliance of a wind turbine’s soil-foundation system was employed by [32] with the use of a lumped parameter model that consists of six uncoupled springs, one along each of the six degrees of freedom. No dashpots were considered and the stiffness coefficients of the generalized spring elements were calculated independently on the seismic excitation frequency. The findings obtained therein verified the sensitivity of the turbine’s tower dynamic characteristics in the SSI phenomena (i.e., reduction in tower’s natural frequencies). Furthermore, the seismic analysis, based on the time domain approach with the use of artificial accelerograms, showed an almost perfect agreement in the response results associated with either the simplified, springs-based substitute model for the SSI or the more accurate BEM (boundary elements method) model, implemented also by [32]. Recently, [33] assesses the response of seismic excitation for Gamesa G52/850 55m hub height, located at Zafarana wind turbine towers farm in Egypt, including SSI using finite element method by OpenSees using pressure dependent multi-yield surface soil constitutive model that verified with experimental work done by [34], the result of this research proved all the previous studies that SSI has an important effect on the dynamic response of the wind tower due to seismic excitation.

III. Finite Element Analysis Using Plaxis 3D

A. *General*

For seismic foundation-ground system analyses, nonlinear constitutive models are needed for the soil and for the pile materials [33]. Plaxis 3D is a three-dimensional finite element program developed specifically for use in geotechnical engineering and design. It is possible to choose from a range of predefined material models, developed for describing soil behavior, the analysis of deformation, stability, groundwater flow and earthquakes in geotechnical engineering.

B. *Interface Element*

In order to simulate the contact between soil and structural units, it is necessary to define interfaces. This is done to specify a lower strength between a structure surface and the soil. Without interface elements, no slipping or gapping is allowed, which in most cases is a non-physical assumption for the interaction between structure and soil. The interface material model is elastic-plastic and based on the Coulomb failure criterion.

C. *Standard Boundary Conditions*

Plaxis assigns general fixities to the boundaries of the model in Fig. 1. The vertical boundaries are by default free in z direction and the lateral direction parallel to the boundary plane, while fixed in the normal direction to the boundary. The top surface is by default free in all directions, while the bottom surface is completely fixed.

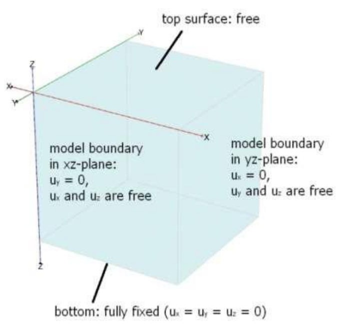

Figure 1. Defult Boundaries in Plaxis 3D

D. *Dynamic Modeling in Plaxis 3D*

1) Dynamic Basics

The basic equation for the time-dependent movement of a volume under the influence of a (dynamic) load is shown in (1):

$$M\, \ddot{u} = C\, \dot{u} + K\, u \qquad (1)$$

Where, M is the mass matrix, u, $\dot{u}$ and $\ddot{u}$ are the displacement, velocity and acceleration vectors, can vary with time, C is the damping matrix and K is the stiffness matrix. The last two terms in (1) (K u = F) correspond to the static deformation. In the matrix M, the mass of the materials (soil + water + any constructions) is taken into account. In Plaxis the mass matrix is implemented as a lumped matrix. The matrix C denotes the damping of material. In reality, damping of material is produced by resistance or by irrecoverable deformations (plasticity or viscosity). As viscosity and plasticity increase, the dissipation of the vibration energy increases. In finite element interpretations, C is frequently expressed as a function of the mass and stiffness matrices [35-36] (Rayleigh damping) presented in (2).

$$C = \alpha R\, M + \beta R\, K \qquad (2)$$

This limits the determination of the damping matrix to the Rayleigh coefficients α_R and β_R. Here, when the contribution of M is dominant (for example, $\alpha_R = 10^{-2}$ and $\beta_R = 10^{-3}$) more of the low frequency vibrations are damped, and when the contribution of K is dominant (for example, $\alpha_R = 10^{-3}$ and $\beta_R = 10^{-2}$) more of the high-frequency vibrations are damped.

2) Dynamic Model Boundaries

For dynamic calculations, the boundaries should in principle be much further away than those for static calculations, because, otherwise, stress waves will be reflected leading to distortions in the computed results. However, locating the boundaries far away requires many extra elements and therefore a lot of extra memory and calculating time. To counteract reflections and avoid spurious waves, Plaxis uses the following dynamic model boundaries.

a) Viscous Boundaries

In opting for viscous boundaries, a damper is used instead of applying fixities in a certain direction. The damper ensures that an increase in stress on the boundary is absorbed without rebounding. The boundary then starts to move. The use of viscous boundaries in PLAXIS is based on the method described by [37]. The normal and shear stress components absorbed by a damper in x -direction are shown in (3) and (4).

$$\sigma_n = -C_1\, \rho\, V_p\, \dot{u}_x \qquad (3)$$

$$\tau = -C_2\, \rho\, V_s\, \dot{u}_y \qquad (4)$$

where ρ is density of material, V_p, V_s are the pressure wave velocity and the shear wave velocity respectively, $\dot{u}_x$ and $\dot{u}_y$ are the normal and shear particle velocities derived by time integration and C_1, C_2 are relaxation factors to develop the influence of absorption. $C_1 = C_2 = 1$ and $C_1=1$, $C_2=0.25$ for normal and shear waves respectively [38].

b) Free-Field and Compliant Base Boundaries

In a free-field boundary, the area is decreases to the interested domain and the free field motion is applied to the boundaries employing free-field elements. A free-field element involves a one-dimensional element in two dimensional problems coupled to the main grid by viscous dashpots shown in Fig. 2. To define the wave propagation in inner elements, the identical mechanical behaviors as the adjacent soil element in the main domain is used. To avoid the reflection of the waves from internal structures (or produced by sources inside the domain), the main domain boundary surrounding by viscous boundaries as shown in Fig. 3 and Fig. 4 [38].

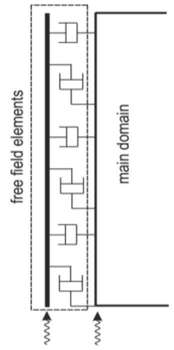

Figure 2. Free field elements [38]

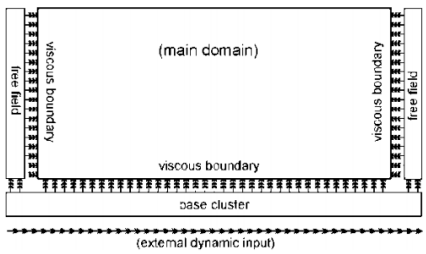

Figure 4. Free field boundary condition with compliant base (no wave reflection at base) [38]

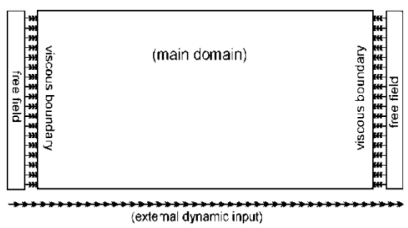

Figure 5. Free field boundary condition with rigid base (wave reflection at base) [38]

The free field motion is transmuted from elements at free field domain to the core area by application of equivalent forces according to (5) and (6). These equations show that how viscous boundaries affect at the boundaries of the model to absorb the reflected internal structures waves [38].

$$\sigma_n = - C_1 \rho V_p (\dot{u}_x^{m} - \dot{u}_x^{ff}) \quad (5)$$

$$\tau = - C_2 \rho V_s (\dot{u}_y^{m} - \dot{u}_y^{ff}) \quad (6)$$

where $\dot{u}^{m}$, $\dot{u}^{ff}$ are the particle velocities in the main grid and in the free-field element respectively and C_1, C_2=1.

As shown in Fig. 4 and Fig. 5, Free-field elements can be attached to the lateral boundaries of the main domain. If the bottom cluster takes into consideration, dynamic excitation input and absorption can be done at the same boundary (at the bottom level of the model) [39]. The equivalent stresses in a compliant base are given by (7) and (8).

$$\sigma_n = - C_1 \rho V_p (\dot{u}_x^{d} - \dot{u}_x^{u}) \quad (7)$$

$$\tau = - C_2 \rho V_s (\dot{u}_y^{d} - \dot{u}_y^{u}) \quad (8)$$

Where $\dot{u}^{u}$ and $\dot{u}^{d}$ are the upward and downward particle velocities, which can be considered as displacement in the element and the main domain, respectively. The compliant base works correctly if the tangential relaxation coefficient C_2 is equal to 1. The reaction of the dashpots is multiplied by a factor 2 since half of the input is absorbed by the viscous dashpots and half is transferred to the main domain. This is the difference between the compliant base and the free field boundary conditions.

3) The Harding Soil Model with Small Strain Stiffness (HSsmall)

This soil constitutive model is the most appropriate soil model in Plaxis 3D that can be used in the dynamic analysis problems. The original Hardening Soil model assumes elastic material behavior during unloading and reloading. Though, the strain levels in which soils can be considered actually elastic, i.e. where they recuperate from applied straining almost totally, is very small. As shear strain increases, the shear modulus stiffness decreases nonlinearly. Plotting soil stiffness against log(strain) yields characteristic S-shaped stiffness reduction curves. Fig. 6 gives an illustration of such a stiffness reduction curve. It outlines also the characteristic shear strains that can be measured near geotechnical structures and the applicable strain ranges of laboratory tests. It turns out that at the minimum value of strain which can be determined in traditional laboratory tests, i.e. triaxle tests and oedometer tests without any advanced instruments, soil stiffness is frequently decreased to less than half its initial value.

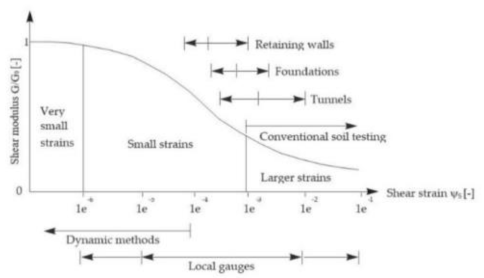

Figure 6. Charactaristics stiffness-strain behavior of soil with typical strain rangs for laboratory [40]

The Hardening Soil model with small-strain stiffness implemented in Plaxis is built on the Hardening Soil model and uses the same input parameters. Actually, there are two extra parameters are required to define the variation of stiffness with strain; the initial or very small-strain shear modulus G_0 and the shear strain level $\gamma_{0.7}$ at which the ratio between the secant shear modulus G_s to G_0 is 0.722 [41].

IV. Model of Vestas V47/660 Wind Turbine Tower

Zafarana wind turbine farms contain three types of wind turbines that distribute along the eight Zafarana wind farms which are Nordex N43/600, Vestas V47/660 and Gamesa G52/850. In this paper, Vestas V47/660 wind turbine tower that located in Zafarana 3 (Soil Class B) and Zafarana 5 (Soil Class C) chosen to be the wind turbine structure which modeled with two different seismic excitations. In the next sections, the model geometry, parameter selection and method of dynamic analysis in Plaxis 3D will be discussed.

A. *Characteristics of Vestas V47/660*

The V47-660 kW has a hub height 45.70m formed of two parts of modular tower with bottom diameter 3.0m and top diameter 2.0m. Fig. 7 shows V47/660 constructed at Zafarana wind farm.

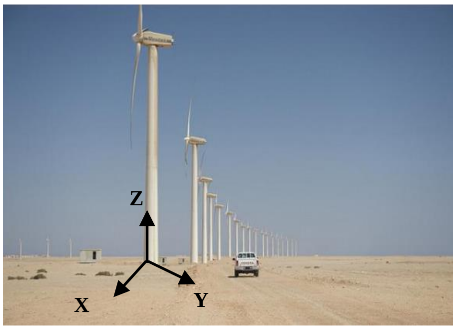

Figure 7. Vestas V47/660 Wind Turbine Tower at Zafarana Wind Farm

The swept area of V47/660 is 1735 m^2, rotor diameter is 47m and speed range is 20 to 28.5 RPM. The weights of the blades, nacelle and hub, rotor and tower are 19kN, 204kN, 72kN and 490kN respectively. The natural frequency of the rotor of the Vestas v47/660 is between 1P and 3P so the value of this frequency is between 0.475 and 1.43 Hz respectively. So there are three types of stiffness for tower and its foundation that may be soft-soft type where its natural frequency is less than 1P, soft-stiff type where the tower and its foundation frequency is between 1P and 3P and the last type is the stiff-stiff type that the tower and its foundation stiffness is more than 3P. For the Vestas v47/660 at Zafarana wind farm, the frequency of the combined turbine, tower and foundation is 0.61Hz +/- 5% that lies between 1P (0.475Hz) and 3P (1.43Hz) so the type of the tower and foundation structure is soft-stiff type [42]. As mentioned before, at the top of the turbine tower there are blades connected with hub, rotor and nacelle. The total load of these elements transferred to act on a point on the top of the tower and moments bout x and y axes. The values of these reactions are 33.3 kN in –Z direction and moment about x-axis is -20 kN.m and about y-axis is 33 kN.m.

B. *Soil Structure Interaction Model*

1) Concept and Geometry

Two main soil models simulate two site conditions in Zafarana 3 (Soil Class B) and Zafarana 5 (Soil Class C) at Zafarana wind turbine farm. For Zafarana 3, the soil consists Clay Stone layer with average V_s (944m/s) extended from ground level till the end of the borehole and geophysical done by [3]. And Zafarana 5 soil formation is 6.0m wadi deposit then Silty Sand layer till end of boring with average V_s (523m/s). To prevent the boundary condition effect, a wide boundary is chosen for soil profile that stated at many previous researches. This boundary depends on the dimension of the foundation of wind turbine tower. So the dimension of raft foundation is 9.00m*9.00m for Vestas V47/660 with 45m tower height as the design of Vestas V47/660 foundation in manual for hub height 37.50 was 8.30m and its thickness was 1.00m. So the boundary of the model lies on a distance that equals to eight times of footing radius/width from right and left which is approximately 35.00m. The final volume of 3D model in Plaxis is 70*70*36 m where (X_{min}=-35m, X_{max}=35m and Z_{min}=-36m). The two models used in the SSI analysis using Plaxis 3D shown in Fig. 8 and Fig. 9.

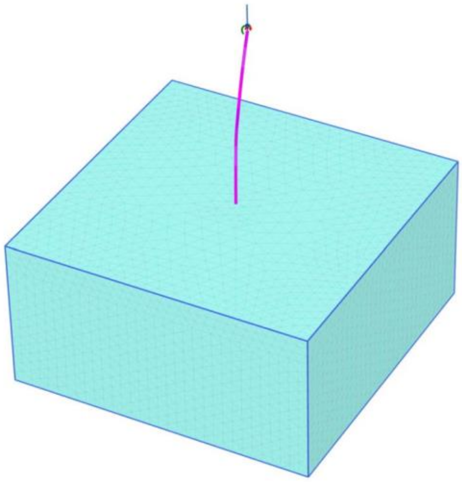

Figure 8. Vistas V47/660 at Zafarana 3 (Soil Class B) in Plaxis 3D

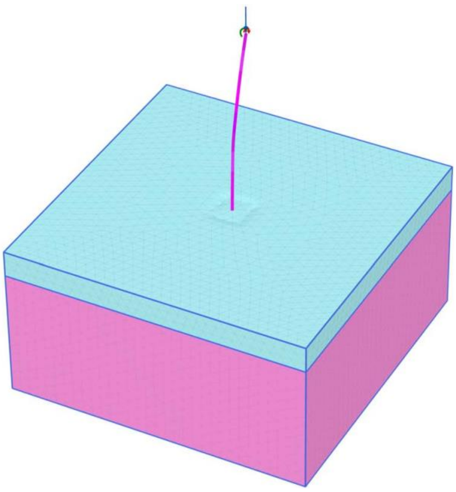

Figure 9. Vistas V47/660 at Zafarana 5 (Soil Class C) in Plaxis 3D

International Journal of Civil and Structural Engineering – IJCSE
Copyright © Institute of Research Engineers and Doctors
Volume 6 : Issue 2 - [ISSN : 2372-3971] - Publication Date: 27 Dec, 2019

2) Soil and Structure Materials

As mentioned before, Harding soil model with small strain (HSsmall) is the best appropriate model in Plaxis that captures the far filed seismic effect so HSsmall model used in this study to define the soil properties. The parameters of HSsmall model for all different soil layers with interface with structure contacting with soil for the two soil classes investigated are illustrated in (TABLE I).

TABLE I. SOIL PARAMETERS IN PLAXIS 3D

Soil Type	Unite	Zafarana 3 Soil Class B	Zafarana 5 Soil Class C	
Identification		*Clay Stone*	*Wadi Deposit*	*Silty Sand*
Drainage type		Drained	Drained	Drained
γ_{unsat}	kN/m^3	23.00	20.00	16.00
γ_{sat}	kN/m^3	23.00	20.00	18.00
Rayleigh α		0.1077	0.09861	0.09861
Rayleigh β		0.4547E-3	0.6853E-3	0.6853E-3
E_{50}^{ref}	kN/m^2	70.00E3	40.00E3	12.50E3
E_{oed}^{ref}	kN/m^2	56.00E3	32.00E3	10.00E3
E_{ur}^{ref}	kN/m^2	210.0E3	120.0E3	37.50E3
power (m)		0.7000	0.9000	1.000
c ref	kN/m^2	200.0	2.000	7.000
(phi)		38.00	37.00	26.00
(psi)		8.000	7.000	0.000
$\gamma_{0.7}$		7.000E-3	0.01800	0.700E-3
G_{0ref}	kN/m^2	218.8E3	140.0E3	42.00E3
Poisson's ratio		0.3000	0.2000	0.2000
p_{ref}	kN/m^2	100.0	100.0	100.0
K_{0nc}		0.3843	0.3982	0.5616
R_{int}		0.9000	0.75	0.8

As stated before that the Vestas tower hub height is 43.70m and it is a modular steel cylindrical tube that its radius varies from 3.00m at bottom to 2.00m at the top. And the weight of the tower is 490 kN and from the unit weight of steel (75.8 kN/m^3) the average thickness of the tower was 0.018m. As a result, nine sections are simulated the tower section. The beam element used to model the tower of Vestas wind turbine as shown in (TABLE II).

TABLE II. MATERIALS PROPERTIES OF VESTAS V47/660 TOWER

Parameter	Name	Tower	Unit
Type of behavior	Type	Elastic: Isotropic	-
Material weight	γ	75.80	kN/m^3
Young's Modulus	E	210.0E6	kN/m^2
Beam type	-	Circular Tube	-
Diameter	*D*	2-3	m
Thickness	*t*	0.018	m
Rayleigh damping	α	0.09522	-
Rayleigh damping	β	3.954E-3	-

For the footing thickness assumed to be 1.00m at the edge of footing and will be 1.20m at the center. Consequently, the footing is modeled as a plate element with three different sections with different thickness 1.05, 1.15 and 1.20. The plate element properties for the three foundation sections presented in (TABLE III).

TABLE III. FOOTING PROPERTY IN PLAXIS 3D

Identification	Unit	Footing-1	Footing-2	Footing-3
Material Type	-	Isotropic	Isotropic	Isotropic
Material weight γ	kN/m^3	25	25	25
Thickness d	m	1.20	1.15	1.05
Young's Modulus E	kN/m^2	22.00E6	22.00E6	22.00E6
Poisson's ratio	ν'_{12}	0.20	0.20	0.20
α and β	-	0.0	0.0	0.0

C. *Earthquake Records*

Two records The Kocaeli, 1999 and Loma Prieta, 1989 were used as input motion that acted at the bottom boundary of SSI model. The Kocaeli recorded at Sakaria station with amax (0.628g) and Loma Prieta recorded at Emeryville station with amax (0.25g). The frequency at peak response Fourier spectrum for Kocaeli, 1999 and Loma Prieta, 1989 is 3.12Hz and 0.684Hz respectively. (TABLE IV) shows the properties of the two records. Since these records were recorded at the ground surfaces and the effect of compliant base boundary in the bottom base, these records scaled to peak ground acceleration (PGA) 0.50g in –Y-direction at the base of the model as in Fig. 10 and Fig. 11.

TABLE IV. EARTHQUAKE RECORDS PROPERTIES

EQ Event/ Location	Date	Source	Recording station	a_{max} g	f (Hz)
The Kocaeli (Turkey)	August 17, 1999	PEER Strong Motion Database	Sakaria recording station	0.628g	3.122
The Loma Prieta (USA)	October 18, 1989	PEER Strong Motion Database	Emeryville recording station	0.25g	0.684

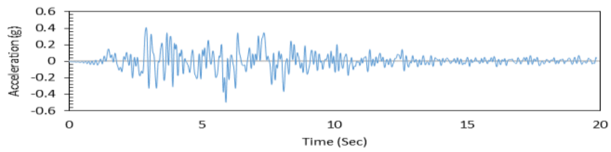

Figure 10. The Kocaeli, 1999 scaled record to 0.50g PGA

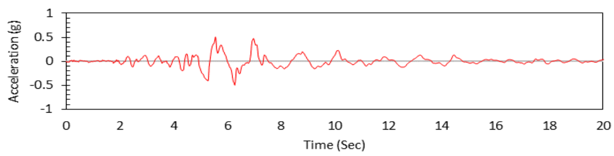

Figure 11. The Loma Prieta, 1989 scaled record to 0.50g PGA

V. Results and Discussion

Hysteretic damping of the soil model assigned to the SSI model using Rayleigh damping formulation and to get Rayleigh coefficients, [43] strategy used and fundamental frequency of soil deposit determined by [44] that equal the average shear wave velocity divided by four times the depth of soil stratum. The response acceleration $a_y(g)$ at center of footing and top of tower and total displacements $U_y(m)$ at top of tower determined and the effect of change in earthquake records and soil types are illustrated below.

A. *Effect of Change in Earthquake*

The results due to two earthquakes of soil class B (fundamental frequency 7.87Hz) are shown below. For the two earthquakes Kocaeli, 1999 and Loma Prieta, 1989, the peak response acceleration at center of footing is 0.11g and 0.13g at 8.53 and 5.59 sec that decreases from (0.25g) with percentage of 56 and 48% respectively as shown in Fig. 12.

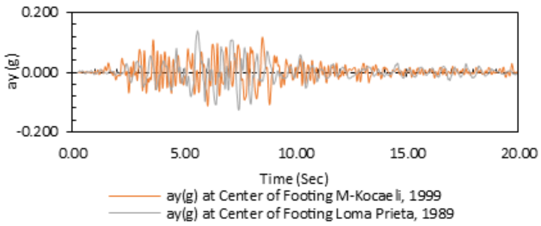

Figure 12. Seismic response $a_y(g)$ at center of footing (Soil Class B)

As the natural frequency of the soil is much higher than the fundamental frequencies of the earthquakes, the peak response acceleration at center of footing is almost the same. On the other hand, at top of tower, the peak response acceleration $a_y(g)$ 0.413g at 9.05sec and 0.61g at 7.63sec and peak response of total displacement $U_y(m)$ is 0.065m at 7.63 sec and 0.135m at 7.07sec for Kocaeli, 1999 and Loma Prieta, 1989 respectively as shown in Fig. 13 and Fig. 14.

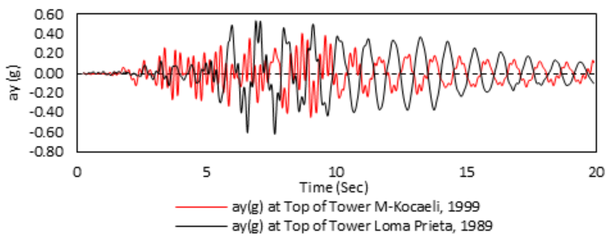

Figure 13. Response $a_y(g)$ at top of tower (Soil Class B)

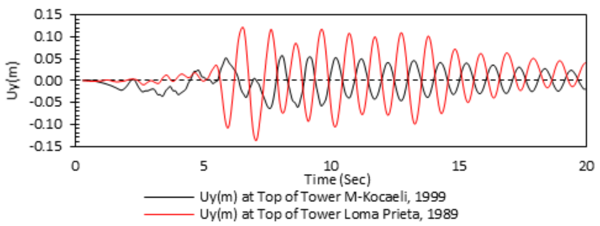

Figure 14. Response $U_y(m)$ at top of tower (Soil Class B)

As the natural frequency of the tower (0.61Hz) is very close to the dominant frequency of Loma Prieta, 1989 (0.648Hz), so its peak response values at top of tower are higher than those for Kocaeli, 1999. The same trend for the peak response values for Soil Class C. For Kocaeli, 1999 and Loma Preita, 1989, the peak response acceleration at center of footing is 0.131g and 0.163g at 8.47sec and 5.55sec with reduction percentage 47.60% and 34.80% respectively due to damping in soil domain. The results discussed before illustrated in Fig. 14.

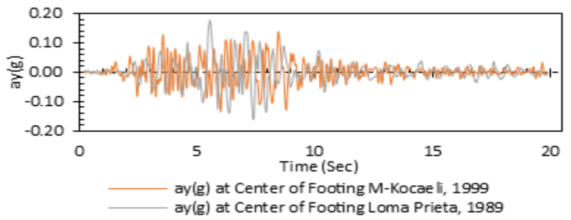

Figure 15. Seismic response $a_y(g)$ at center of footing (Soil Class C)

For Kocaeli, 1999 earthquake, the peak response acceleration and total displacement at top of tower are 0.55g and 0.10m at 8.65 and 8.76 sec. In addition to, for Loma Preita, 1989, these peak response values are 0.783g and 0.217m at 7.65 and 7.12sec as shown in Fig. 16 and Fig. 17.

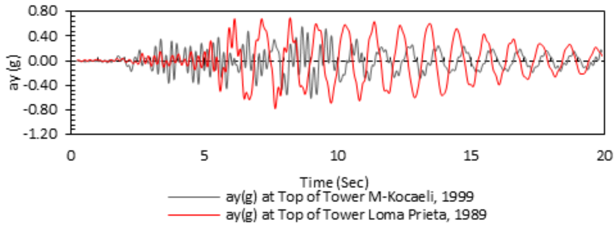

Figure 16. Response $a_y(g)$ at top of towr (Soil Class C)

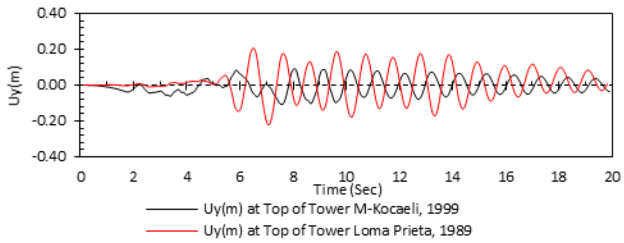

Figure 17. Response $U_y(m)$ at top of tower (Soil Class C)

B. *Effect of Change in Soil Types*

The peak seismic response acceleration $a_y(g)$ at center of footing due to Kocaeli, 1999 is 0.11g and 0.131g for Soil Class B and Soil Class C respectively as presented in Fig. 18. These values are very close together that is meant there isn't any significant difference in the peak response.

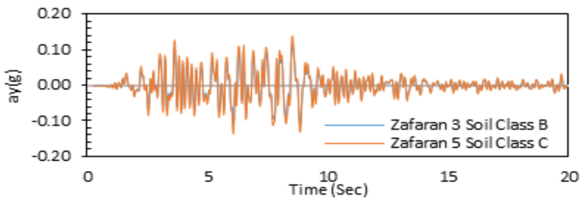

Figure 18. $a_y(g)$ at center of footing for soil classes (*Kocaeli, 1999)*

For the same earthquake record, the peak response acceleration $a_y(g)$ and peak total displacement $U_y(m)$ are 0.413g, 0.55g and 0.065m, 0.116m for Soil Class B and Soil Class C respectively as figured in Fig. 19 and Fig. 20. The results show that as the soil type is softer, the response of the tower is bigger and including SSI in design becomes essential.

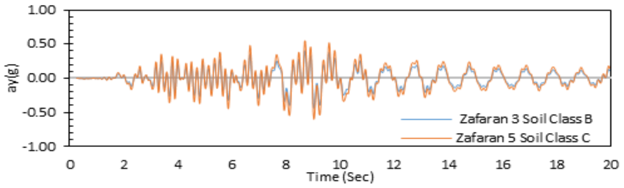

Figure 19. $a_y(g)$ at top of tower for soil classes (*Kocaeli, 1999)*

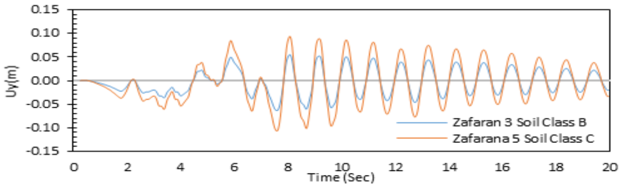

Figure 20. $U_y(m)$ at top of tower for soil classes (*Kocaeli, 1999)*

Similary, dut to Loma Prieta, 1989 record, the peak response acceleration ay(g) at center of footing is very close for Soil Class B and Soil Class C as shown in Fig. 21, where the peak values are 0.13g and 0.163g respectively.

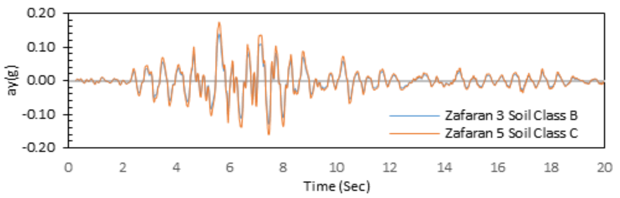

Figure 21. $a_y(g)$ at center of footing for soil classes(*Loma Prieta, 1989)*

At the top of tower, the peak response acceleration ay(g) and total displacement Uy(m), due to Loma Prieta, 1999, for Soil Classes B and C, are 0.61g, 0.783g and 0.135m, 0.217m respectively as in Fig. 22 and Fig. 23. The results proved the previous findings for Kocaeli, 1999.

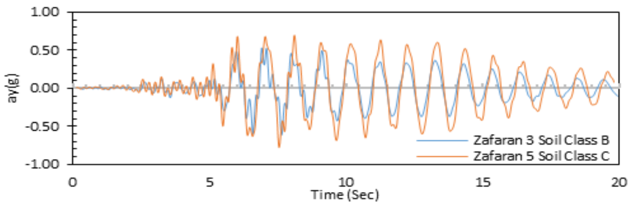

Figure 22. $a_y(g)$ at top of tower for soil classes (*Loma Prieta, 1989)*

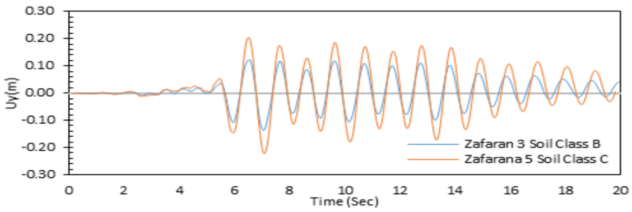

Figure 23. $U_y(m)$ at top of tower for soil classes (*Loma Prieta, 1989)*

VI. Conclusions

In this study, Vestas V47/660 wind turbine tower located at Zafarana wind turbine farm in Egypt simulated by using finite element method to assess the effect of dynamic soil structure interaction on the dynamic response of tower and its foundation due to two earthquake records. The previous results concluded that:

1- The effect of earthquake frequency change has not a significant effect on the peak response acceleration $a_y(g)$ at the center of tower footing for soil classes B and C.
2- Regarding to the tower, the change of earthquake frequency has a significant effect on the peak response displacement at the top of tower. As the frequency of the earthquake is close to natural frequency of the tower, the peak response displacement increases dramatically.
3- As soil natural frequency, fundamental frequency of earthquake and natural frequency of tower are close together, the peak response of footing and tower increases sharply as the resonant phenomena occurred and a large deformations cause structural failure.
4- Complicated 3D model including dynamic soil structure interaction is very essential to capture the dynamic interaction for all system (Soil, foundation and structure) especially in such special structure like wind turbine towers.

It is noted that, this study just covers only one onshore wind turbine tower that hasn't a big height and the aerodynamic loads of blades didn't take into consideration so, it is recommended to take them in the future research. Also, the dynamics SSI using Plaxis 3D needs to be verified experimentally using full scale shaking table test and study the effect of SSI on soil softer than soil classes B and C.

Acknowledgment

The authors acknowledge Dr. Sherif Abdelbaki, Former Assistant Lecture, Cairo University (Fayoum Branch) and owner of Active Brains Consulting Group (ABCG) to provide the license of Plaxis 3D, 2017 that used in this research to perform dynamic soil structure interaction analysis.

References

[1] Timilsina, G.R. and A. Shrestha, An overview of global markets and policies, in The Impacts of Biofuels on the Economy, Environment, and Poverty. 2014, Springer. p. 1-14.
[2] Patil, A., S. Jung, and O.-S. Kwon, Structural performance of a parked wind turbine tower subjected to strong ground motions. Engineering Structures, 2016. 120: p. 92-102.
[3] Yagi, Y. and H. Kamal, Implementation of integrated multi-channel analysis of surface waves and waveform inversion techniques for seismic hazard estimation. Arabian Journal of Geosciences, 2016. 9(4): p. 322.
[4] Veletsos, A.S. and J.W. Meek, Dynamic behaviour of building- foundation systems. Earthquake Engineering & Structural Dynamics, 1974. 3(2): p. 121-138.
[5] Banerjee, P.K. and R. Butterfield, Dynamic behaviour of foundations and buried structures. 1987: Elsevier Applied Science.

[6] V, J.T.a.S.G., Soil Structure Interaction on 100m Tall Industrial Chimney under Seismic Load. International Journal of Engineering Research & Technology (IJERT), 2014. 3(8): p. 782-789.

[7] Dixit, J., D. Dewaikar, and R. Jangid, Free field surface motion at different site types due to near-fault ground motions. ISRN Geophysics, 2012. 2012.

[8] Bajaj, K., J.T. Chavda, and B.M. Vyas. Seismic behaviour of buildings on different types of soil. in Proceedings of Indian Geotechnical Conference. 2013.

[9] Athanasopoulos, G., P. Pelekis, and G. Anagnostopoulos, Effect of soil stiffness in the attenuation of Rayleigh-wave motions from field measurements. Soil Dynamics and Earthquake Engineering, 2000. 19(4): p. 277-288.

[10] Bolisetti, C., A.S. Whittaker, and J.L. Coleman, Frequency-and Time-Domain Methods in Soil-Structure Interaction Analysis. 2015, Idaho National Lab.(INL), Idaho Falls, ID (United States).

[11] Jaya, K. and A.M. Prasad, Embedded foundation in layered soil under dynamic excitations. Soil Dynamics and Earthquake Engineering, 2002. 22(6): p. 485-498.

[12] Adhikari, S. and S. Bhattacharya, Vibrations of wind-turbines considering soil-structure interaction. Wind and Structures, 2011. 14(2): p. 85.

[13] Butt, U.A. and T. Ishihara, Seismic load evaluation of wind turbine support structures considering low structural damping and soil structure interaction. European wind energy association annual event, 2012: p. 16-19.04.

[14] Harte, M., B. Basu, and S.R. Nielsen, Dynamic analysis of wind turbines including soil-structure interaction. Engineering Structures, 2012. 45: p. 509-518.

[15] Hongwang, M. Seismic analysis for wind turbines including soil-structure interaction combining vertical and horizontal earthquake. in 15th World Conference on Earthquake Engineering, Lisbon, Portugal. 2012.

[16] Kausel, E., Early history of soil–structure interaction. Soil Dynamics and Earthquake Engineering, 2010. 30(9): p. 822-832.

[17] Ishihara, T. and M. Sarwar. Numerical and theoretical study on seismic response of wind turbines. in European wind energy conference and exhibition. 2008.

[18] Witcher, D., Seismic analysis of wind turbines in the time domain. Wind Energy: An International Journal for Progress and Applications in Wind Power Conversion Technology, 2005. 8(1): p. 81-91.

[19] Prowell, I., et al. Shake table test of a 65 kW wind turbine and computational simulation. in 14th World Conference on Earthquake Engineering, Beijing, China. 2008.

[20] Luco, J.E., Soil-structure interaction effects on the seismic response of tall chimneys. Soil Dynamics and Earthquake Engineering, 1986. 5(3): p. 170-177.

[21] Moghaddasi, M., et al., Effects of soil–foundation–structure interaction on seismic structural response via robust Monte Carlo simulation. Engineering Structures, 2011. 33(4): p. 1338-1347.

[22] Prowell, I., A. Elgamal, and J. Lu, Modeling the influence of soil structure interaction on the seismic response of a 5 MW wind turbine. 2010.

[23] Bazeos, N., et al., Static, seismic and stability analyses of a prototype wind turbine steel tower. Engineering structures, 2002. 24(8): p. 1015-1025.

[24] Lavassas, I., et al., Analysis and design of the prototype of a steel 1-MW wind turbine tower. Engineering structures, 2003. 25(8): p. 1097-1106.

[25] Prowell, I., et al., Experimental and numerical seismic response of a 65 kW wind turbine. Journal of Earthquake Engineering, 2009. 13(8): p. 1172-1190.

[26] Kühn, M.J., Dynamics and design optimisation of offshore wind energy conversion systems. 2001: DUWIND, Delft University Wind Energy Research Institute.

[27] Bush, E. and L. Manuel. Foundation models for offshore wind turbines. in 47th AIAA aerospace sciences meeting including the new horizons forum and aerospace exposition. 2009.

[28] Liingaard, M., Dynamic behaviour of suction caissons. 2006, Aalborg University, Department of Civil Engineering, Division of Water and Soil.

[29] Larsen, T.J., H.A. Madsen, and K. Thomsen, Investigation of stability effects of an offshore wind turbine. The new aeroelastic code HAWC2. Windtech International, 2006. 2(March): p. 33-35.

[30] Al Satari, P.M. and S.S. Hussain. Vibration Based Wind Turbine Tower Foundation Design Utilizing Soil- Foundation- Structure Interaction. in AIP conference proceedings. 2008. AIP.

[31] AlHamaydeh, M. and S. Hussain, Optimized frequency-based foundation design for wind turbine towers utilizing soil–structure interaction. Journal of the Franklin Institute, 2011. 348(7): p. 1470-1487.

[32] Taddei, F. and K. Meskouris, Seismic analysis of onshore wind turbine including soil-structure interaction effects, in Seismic Design of Industrial Facilities. 2014, Springer. p. 511-522.

[33] Zayed, M., et al. Response of A 850 KW Wind Turbine Including Soil-Structure Interaction During Seismic Excitation. in International Congress and Exhibition" Sustainable Civil Infrastructures: Innovative Infrastructure Geotechnology". 2018. Springer.

[34] Saudi, G., Experimental modal identification of full-scale wind turbine towers, in 7th International Operational Modal Analysis Conference. 10-12 May 2017: Ingolstadt, Germany.

[35] Zienkiewicz, O. and J. Wu, *Incompressibility without tears—how to avoid restrictions of mixed formulation.* International Journal for numerical methods in engineering, 1991. **32**(6): p. 1189-1203.

[36] Hughes, T.J. and L.P. Franca, *A new finite element formulation for computational fluid dynamics: VII. The Stokes problem with various well-posed boundary conditions: symmetric formulations that converge for all velocity/pressure spaces.* Computer Methods in Applied Mechanics and Engineering, 1987. **65**(1): p. 85-96.

[37] Lysmer, J. and R.L. Kuhlemeyer, *Finite dynamic model for infinite media.* Journal of the Engineering.

[38] Galavi, V., A. Petalas, and R. Brinkgreve, *Finite element modelling of seismic liquefaction in soils.* Geotechnical Engineering Journal of the SEAGS & AGSSEA, 44 (3), 2013.

[39] Joyner, W.B. and A.T. Chen, *Calculation of nonlinear ground response in earthquakes.* Bulletin of the Seismological Society of America, 1975. **65**(5): p. 1315-1336.

[40] Atkinson, J. and G. Sallfors. Experimental determination of soil properties. General Report to Session 1. in Proc. 10th ECSMFE, Florence. 1991.

[41] Brinkgreve, R., et al., Plaxis 2014. PLAXIS bv, the Netherlands, 2016

[42]Vestas V47/660 kW Wind Tubine Tower Techincal Manual, 1997.

[43] Hudson, M., I. Idriss, and M. Beirkae, *QUAD4M User's Manual.".* A computer program to evaluate the seismic response of soil structures using finite element procedures and incorporating a compliant base, 1994.

[44] Kramer, S.L.: Geotechnical earthquake engineering. In: Prentice-Hall International Series in Civil Engineering and Engineering Mechanics. Prentice-Hall, New Jersey (1996)

About Author (s):

Prof. Dr. Gihan Elsyed Abdelrahman

The change of earthquake frequency has not a significant effect on the seismic response at center of tower footing for soil class B and soil class C

Dr. Youssef Gomaa Youssef

Regarding to the tower, the change of earthquake frequency has a significant effect on the peak response displacement at the top of tower

Dr.Mohamed Hussien Abdelaziz

As soil natural frequency, frequency of earthquake and natural frequency of tower are close together, the peak response of footing and tower increases

Eng.Khaled Ibrahim Mohamed

Complicated 3D model including dynamic soil structure interaction is very essential to capture the dynamic response for wind turbine towers